Large impurity effects in rubrene crystals: First-principles calculations

L. Tsetseris
Department of Physics, Aristotle University of Thessaloniki, GR-54124 Thessaloniki, Greece
and Department of Physics and Astronomy, Vanderbilt University, Nashville, Tennessee 37235, USA

S. T. Pantelides
Department of Physics and Astronomy, Vanderbilt University, Nashville, Tennessee 37235, USA
and Oak Ridge National Laboratory, Oak Ridge, Tennessee 37831, USA
(Received 5 September 2008; published 22 September 2008)

Carrier mobilities of rubrene films are among the highest values reported for any organic semiconductor. Here, we probe with first-principles calculations the sensitivity of rubrene crystals on impurities. We find that isolated oxygen impurities create distinct peaks in the electronic density of states consistent with observations of defect levels in rubrene and that increased O content changes the position and shape of rubrene energy bands significantly. We also establish a dual role of hydrogen as individual H species and H impurity pairs create and annihilate deep carrier traps, respectively. The results are relevant to the performance and reliability of rubrene-based devices.

DOI: 10.1103/PhysRevB.78.115205 PACS number(s): 72.80.Le, 71.20.Rv, 71.55.Ht

Rubrene (Rub) has emerged[1–13] in recent years as a very promising system for applications in organic electronics, mainly because rubrene films currently hold the record of high carrier mobilities among organic semiconductors. Rubrene (5,6,11,12-tetraphenyl-tetracene) molecules comprise four phenyl groups that are attached on the sides of a tetracene back bone (TBB). The molecules form orthorhombic crystals,[14,15] so that large portions of the tetracene units of neighboring molecules face each other in parallel (Fig. 1). This type of packing enhances the overlap between molecular orbitals facilitating intermolecular hopping of carriers.

Oxygen and hydrogen are ubiquitous impurities in electronic materials. In Si-based devices, oxygen is generally a benign impurity;[16] whereas hydrogen has beneficial effects, in that it passivates unwanted defects but can also mediate defect creation.[17] In the case of organic semiconductors, the noncovalent bonding character that provides flexibility to molecular crystals may at the same time facilitate the insertion of impurities that affect the properties of the host matrix. In the case of rubrene crystals, experiments have indeed attributed changes in their electronic properties[18–22] to the presence of oxygen-related impurities. Similar H and O effects are typical for other prototype organic semiconductors, such as pentacene.[23,24] Given the clear significance of defects, the elucidation of the atomic-scale details of impurity insertion in organic semiconductors and specifically in rubrene can play a key role in the optimization of related electronic devices.

In this paper, we use first-principles calculations to examine the effect of oxygen and hydrogen insertion on the properties of rubrene crystals. We first identify the atomic-scale structural details and stability of defect configurations with isolated species and impurity pairs thus resolving questions posed by pertinent experimental data. We then examine the effect of the most stable structures on the electronic properties of rubrene and we identify prominent impurity-induced changes that include formation and annihilation of carrier traps and variations in the energy-band gap, the width, and the shape of the valence and conduction bands of the organic semiconductor. Overall, the results are relevant both for the dilute limit where impurities manifest experimentally[19,20] as isolated defect levels, and for the opposite regime of heavily oxidized films produced either by aging or through intentional defect engineering.

The results were obtained using density-functional theory (DFT) calculations, with a local-density approximation (LDA) exchange-correlation (xc) functional,[25] plane waves as a basis set (the energy cutoff was set at 400 eV), and ultrasoft pseudopotentials to represent the ionic cores[26] as implemented in the code VASP.[27] We used either the unit cell[15] with two rubrene molecules or a supercell with four molecules and with lattice vectors (13.43,−3.5965,0), (0,14.386,0), and (0,0,14.433) in Å. In particular, the majority of the calculations on the energetics of impurity insertion was performed with the latter large four-molecule supercells. Total-energy calculations for these supercells employed $2\times2\times2$ k grids and the Monkhorst-Pack method for Brillouin-zone sampling.[28] Electronic density of states

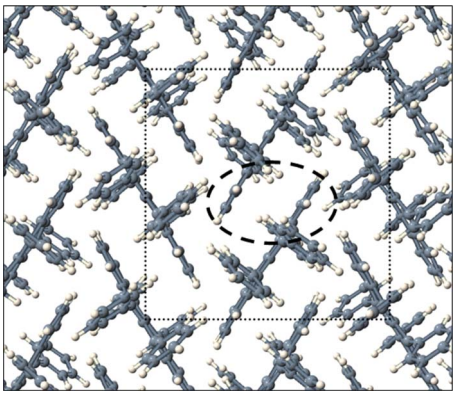

FIG. 1. (Color online) A rubrene crystal with the region of parallel alignment between the tetracene back bones of neighboring molecules enclosed in an ellipse. The dotted line shows the supercell used for the study of impurities in rubrene. (C: gray and H: white spheres)

TABLE I. Formation energies (E_f) for O and H impurities in rubrene based on Eq. (1). Positive (negative) E_f indicate energy gain (penalty) for the formation of the impurity. TBB is the tetracene backbone of rubrene, and x is the number of impurities.

x impurity	Structure	Description	E_f (eV)
1-O	Epoxy	Figure 2(a)	0.9
1-O	Epoxy	On phenyl group	0.3
1-O	Epoxy	On *C*7-*C*8 of Fig. 2(a)	0.6
1-O	Epoxy	On *C*8-*C*9 of Fig. 2(a)	0.8
2-O	Epoxy	Figure 2(b)	2.2
2-O	Epoxy	On phenyl group	1.7
2-O	Epoxy	On vicinal molecules	1.9–2.2
2-O	Peroxides	Similar to Fig. 2(c)	<1.1
1-H		Figure 5(a)	0.1
1-H		On sites 2–8 of Fig. 5(a)	<−0.4
2-H		Figure 5(b)	1.5
2-H		Opposite sides of TBB	1.1
2-H		On *C*1 and *C*1″ of Fig. 5(b)	<−0.6

(DOS) for the four-molecule supercells used larger $6\times6\times6$ k meshes (we checked for DOS convergence against smaller $m\times m\times m$ k grids with $m=2$, 3, and 4) and the tetrahedron sampling method.[29] The DOS calculations for rubrene crystals with large oxygen content employed the smaller unit cells with two molecules, $8\times8\times8$ k meshes, and the tetrahedron method.

In Table I we give the formation energies (E_f) of O and H defects in various configurations. For an O impurity we have

$$E_f = E_i - E^0_{\text{Rubrene}} - \frac{x}{2}E_{O_2}, \tag{1}$$

where x is the number of O species, E_i, E^0_{Rubrene}, and E_{O_2} are the absolute total energies of the impurity configuration of the four-molecule rubrene supercell and of an O_2 molecule, respectively. For a hydrogen impurity the formula is the same except that the total energy E_{H_2} of an H_2 molecule takes the place of E_{O_2}.

We examined an extensive number of atomic O impurity configurations in a rubrene crystal varying the *C* site for O attachment, as well as the geometry of the defect. The most stable structure of the defective molecule shown in Fig. 2(a) is an epoxy group that comprises an O impurity and two Rub C atoms in a triangular bonding pattern. The incorporation of O from O_2 molecules into epoxy structures in Rub crystals leads to a decrease in energy by 0.28–0.92 eV depending on which *C* sites participate in the epoxy bonding.

Oxygen species normally enter organic semiconductors from the gaseous phase and for this reason, pairs of oxygen impurities in Rub are expected to play a prevalent role. Indeed, experiments find that oxygen molecules react with Rub[18–22] and that in certain cases, these oxidation reactions give rise to levels[19,20] about 0.25 eV above the valence-band maximum (VBM) of the crystal. Based on the expected high reactivity of the *C* sites that link the TBB to a phenyl group,

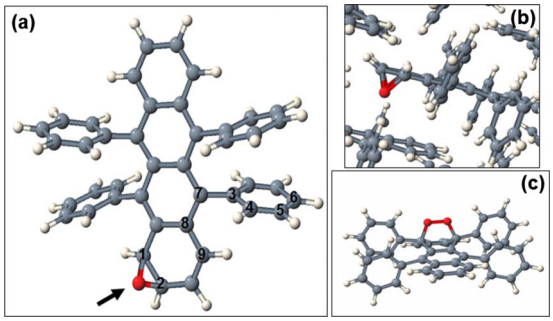

FIG. 2. (Color online) Oxygen impurities in rubrene (Rub): Most stable configuration (epoxy groups) of (a) single O and (b) O pair. Similar structures on the other numbered *C* sites have higher energies. (c) Endoperoxide in a Rub molecule. The energy of (c) is 1.1 eV higher than that of (b). In (a) and (c), only the defective molecule of a Rub crystal is shown for clarity. [C: gray, O: dark gray (red), and H: white spheres]

there have been suggestions[4,19,20] that the dominant O defects in Rub are endoperoxide structures of the form of Fig. 2(c).

We examined the relative stability of a large number of pairs of O species in rubrene including several variants of endoperoxides. We found that the most stable configuration is in fact a pair of proximal epoxy groups that are located, as shown in Fig. 2(b), in the area where two neighboring molecules face off in parallel (dashed ellipse of Fig. 1). In comparison to this epoxy defect, the endoperoxide of Fig. 2(c) lies 1.1 eV higher in energy. Other stable O-O defects include epoxy variants whose energies are 0.1–0.5 eV higher than that of Fig. 2(b) and which comprise two epoxy groups on TBBs of neighboring Rub molecules or on side phenyl groups.

The stabilization of oxygen species in the form of proximal epoxy groups has a profound effect on the electronic properties of rubrene. As shown in Fig. 3, for an O concentration of one epoxy pair per four rubrene molecules, i.e., two O atoms per 168 C atoms, the DOS of the defective

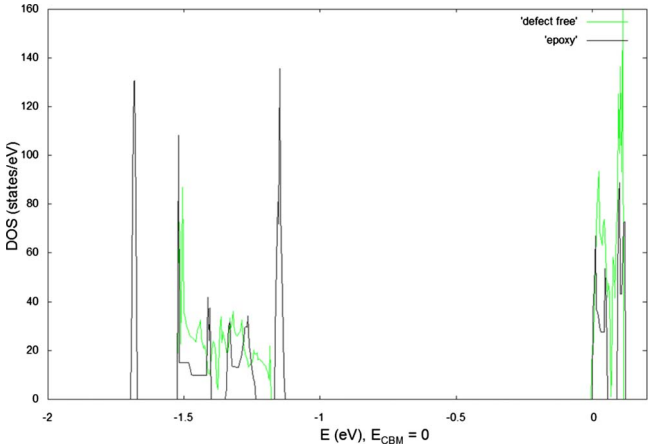

FIG. 3. (Color online) Effects of epoxy pairs on the DOS of Rub. Dark (black) and light (green) lines for a configuration of one epoxy pair per four Rub molecules [Fig. 2(b)] and defect-free Rub, respectively. The zero of energy is set at the conduction-band minimum (CBM).

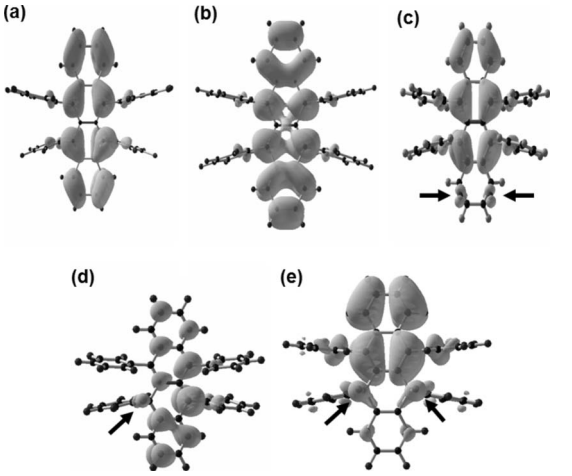

FIG. 4. Amplitude of the HOMO for a rubrene molecule with (a) no impurities, (c) an epoxy pair [Fig. 2(b)], (d) a hydrogen atom [Fig. 5(a)], and (e) a pair of H impurities [Fig. 5(e)] (the arrows show the impurities). (b) Depicts the LUMO of defect-free rubrene.

configuration exhibits major deviations from the DOS of the ideal defect-free case. In particular, the valence band splits in four disjoint parts including a distinct peak at the top that lies about 0.12 eV above the rest of the band. Even though the large required computational power excludes the possibility to extend the calculations to even lower O concentrations and examine the behavior of this peak in the dilute limit, the results of Fig. 3 suggest that the epoxy pair is a likely candidate to explain the observed defect level that has been measured[19,20] at about 0.25 eV above the valence-band maximum of rubrene.

In addition to the appearance of defect levels in the dilute limit, an important issue is the evolution of the properties of rubrene for increased oxygen content. We have probed the DOS for a varying number of epoxy pairs specifically with one, two, and three epoxy pairs per two Rub molecules of the experimental unit cell.[15] The deviations from the pristine Rub DOS are even more dramatic than the ones shown in Fig. 3, and in the latter two cases a substantially larger energy-band gap (1.84 and 1.87 eV, respectively) is obtained. Moreover, the width of the valence band narrows to 0.19 eV for the second case, and in the third case of six epoxy groups, it becomes a depleted narrow peak with two electrons and a width of 0.02 eV.

Figure 4 depicts the amplitude of the highest-occupied (HOMO) and lowest-unoccupied (LUMO) orbitals for Rub molecules and the HOMO for Rub with an epoxy pair. The impurities change the wave function considerably at exactly that part of rubrene, which facilitates carrier hopping and band formation. Significant changes in the bands can then be expected, and when the O content increases, carrier hopping is hindered significantly leading to distortion of the valence band and the widening of the band gap.

We should note that due to well-known limitations of the DFT-LDA functionals, the theoretical band gap (1.19 eV) of pristine Rub is significantly lower than the experimental[19,21] value of 2.3 eV and similar relations are expected for the other band gaps reported here. A more elaborate approach

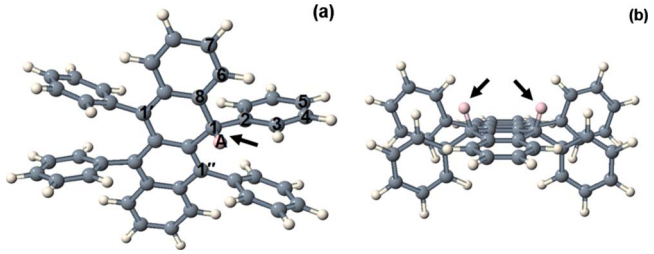

FIG. 5. (Color online) H defects in a Rub crystal: (a) an atomic H impurity at a C atom that links the Rub tetracene back bone to a side phenyl group. (b) pair of vicinal H defects of type (a) located in opposite sites of the same ring of the tetracene back bone. For clarity, the host crystal around the defective molecule is omitted. [C: gray, H: white spheres, extra H: light gray (pink) spheres]

based on the so-called *GW* approximation, which calculates the self-energy from the Green function *G* and the screened interaction *W*, can limit the extent of the DFT band-gap error and improve the accuracy in the positions of unoccupied energy levels, but at present its use is computationally taxing for large supercells. Actually, the relative change in the energy-band gaps and the trend of increase for larger oxygen content, as well as the important features of the results that pertain to variations of the width and shape of the occupied valence bands, are not affected by the band-gap problem of DFT.

We now turn our attention to hydrogen impurities in rubrene crystals. We considered all possible *C* sites for the attachment of atomic H on a rubrene molecule. In the most stable configuration shown in Fig. 5(a), the extra H atom (H_A) binds to one of the TBB C atoms that links the tetracene unit to a side phenyl group. H_A provides an additional bond for the TBB C atom changing its hybridization type away from sp^2 and closer to sp^3. Accordingly, H_A and the associated phenyl group rotate slightly to allow for bond angles that are closer to a tetrahedral arrangement. In particular, using the numbers and indices of the relevant atoms in Fig. 5, the $C2$-$C1$-H_A, H_A-$C1$-$C8$, and $C2$-$C1$-$C8$ angles are equal to 105.9°, 104.8°, and 115.4°, respectively. When the extra H hops from $C1$ to $C6$ or $C7$, the energy increases by 0.52 and 0.62 eV, respectively, and this increase is even larger (1.0–1.4 eV) when H_A is attached at atoms $C2$-$C5$ of the phenyl group. The transformation of an sp^2 hybridization site to an sp^3 type in the case of Fig. 5(a) disrupts the π bonding structure as shown in Fig. 4 for the HOMO of rubrene with a H impurity. Similar to other acene-based systems, such as pentacene,[23,24] new energy levels appear then in the band gap of a rubrene crystal, and the corresponding DOS shown in Fig. 6 demonstrates that atomic H impurities induce distinct peaks at about 0.67 eV above the valence-band maximum.

When two impurity H atoms coexist on the same rubrene molecule, several configurations of stable defect complexes are possible. The lowest energy H defect pair comprises two vicinal interstitial H atoms attached in $C1$ and $C1'$ of Fig. 5(a). The formation of this defect depicted in Fig. 5(b) as a product of absorption of an H_2 molecule is an exothermic reaction with an energy gain of 1.5 eV. The H-H pair has also a binding energy of 1.28 eV against dissociation to isolated

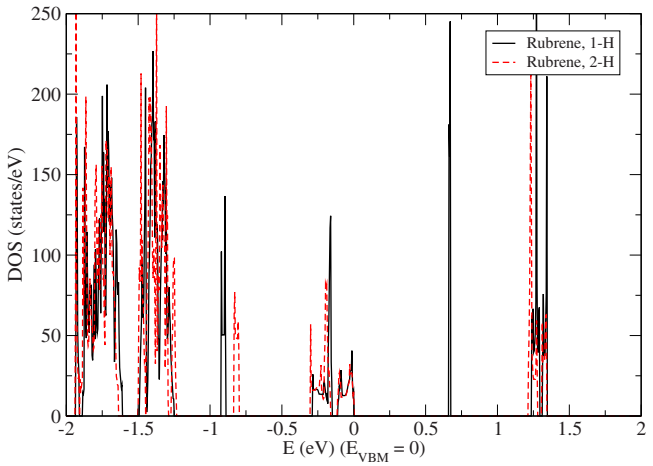

FIG. 6. (Color online) Electronic density of states of Rub H impurities in configurations 1-H (solid line) and 2-H [dashed (red) line] of Fig. 5(a) and Fig. 5(b), respectively. There is one defect per four Rub molecules and the zero of energy is set at the VBM. The 1-H impurity forms deep traps about 0.67 eV above the VBM.

H impurities of the type of Fig. 5(a). This mutual trapping of H impurities is an especially important process because as shown in Fig. 6, the formation of a H pair annihilates the deep energy levels associated with isolated H impurities.

Comparing the HOMO's of Fig. 4(d) for a rubrene molecule with one H impurity with the HOMO [Fig. 4(a)] and the LUMO [Fig. 4(b)] of a defect-free molecule, we note that the symmetry of the defective HOMO does not resemble either the original HOMO or LUMO. For this reason, one can expect that the induced energy level will lie away from the edges of the valence and conduction bands consistent with the appearance of a deep gap level. In contrast, the HOMO of a rubrene molecule with two H impurities [Fig. 4(e)] resembles a large portion of the defect-free HOMO, and the effect of the impurity on the DOS may be expected to relate to changes on or close to the rubrene bands similar to the case of a pair of O impurities.

There are several other possibilities of vicinal H pairs. One stable structure with an energy gain of 1.1 eV compared to H_2 in vacuum comprises two H_A impurities at $C1$ and $C1'$ sites but on opposite sides of the TBB plane. We also examined the stability of pairs with H atoms at the vicinal TBB atoms $C1$ and $C1''$. In this case, the incorporation of the H pair from an H_2 molecule in vacuum is an endothermic reaction with energy penalties of 0.6 and 0.8 eV when both H atoms are on the same TBB side or in opposite TBB sides, respectively.

Rubrene, as a typical organic semiconductor, is characterized by two regimes in terms of mobilities. At high temperatures, mobility is controlled by polaron hopping, and theoretical studies[30] have examined key pertinent issues, such as the reorganization energy of rubrene molecules. The effect of polarons diminishes at lower temperatures, and the role of defects and impurities on carrier transport becomes dominant bearing similarities to inorganic semiconductors. However, we should stress that the enhanced role on electronic properties of localized regions, such as the ellipse of Fig. 1, sets crystalline rubrene apart from traditional bulk materials such as Si, and maximizes the effect of any impurities that show a preference for this particular part of the structure.

The results of the present study are important for the operation of rubrene-based devices as the impurity effects described above have a direct impact on the electronic and transport properties of transistors and optoelectronic systems, as for example, detailed in the case of bias-stressed pentacene films.[31] Impurities may enter organic films during growth, or they can be introduced gradually under long-term operation resulting in degradation and aging of devices. On the other hand, the systematic variation of the energy-band gap and bandwidths with the increase in oxygen content suggests that the achievement of controlled layer-by-layer oxidation of rubrene films could open the way for innovative defect engineering of rubrene-based devices. The details of oxidation kinetics and mechanisms that may enable the selective growth of rubrene films similar to pentacene[32] will be considered elsewhere.

In summary, we have identified, based on first-principles calculations, several prominent impurity effects in rubrene crystals. We have ascribed a dual role to H impurities since they can both form and annihilate carrier traps. We have also found that oxygen species can induce distinct peaks in the electronic density of states and cause large changes in the energy-band gap, shape, and width of rubrene bands.

We acknowledge support by the William A. and Nancy F. McMinn Endowment at Vanderbilt University and by DOE Grant No. DEFG0203ER46096. The calculations were performed at ORNL's Center for Computational Sciences.

[1] V. Podzorov, E. Menard, A. Borissov, V. Kiryukhin, J. A. Rogers, and M. E. Gershenson, Phys. Rev. Lett. **93**, 086602 (2004).
[2] V. C. Sundar, J. Zaumseil, V. Podzorov, E. Menard, R. L. Willett, T. Someya, M. E. Gerzhenson, and J. A. Rogers, Science **303**, 1644 (2004).
[3] C. Goldmann, S. Haas, C. Krellner, K. P. Pernstich, D. J. Gundlach, and B. Batlogg, J. Appl. Phys. **96**, 2080 (2004).
[4] V. Podzorov, V. M. Pudalov, and M. E. Gershenson, Appl. Phys. Lett. **85**, 6039 (2004).
[5] V. Podzorov, E. Menard, J. A. Rogers, and M. E. Gershenson, Phys. Rev. Lett. **95**, 226601 (2005).
[6] V. Podzorov and M. E. Gershenson, Phys. Rev. Lett. **95**, 016602 (2005).
[7] N. Stingelin-Stutzmann, E. Smits, H. Wondergem, C. Tanase, P. Blom, P. Smith, and D. de Leeuw, Nat. Mater. **4**, 601 (2005).
[8] R. Zeis, C. Besnard, T. Siegrist, C. Schlockermann, X. Chi, and C. Kloc, Chem. Mater. **18**, 244 (2006).
[9] I. N. Hulea, S. Fratini, H. Xie, C. L. Mulder, N. N. Iossad, G. Rastelli, S. Ciuchi, and A. F. Morpurgo, Nat. Mater. **5**, 982 (2006).

[10] H. Najafov, I. Biaggio, V. Podzorov, M. F. Calhoun, and M. E. Gershenson, Phys. Rev. Lett. **96**, 056604 (2006).
[11] T. Takahashi, T. Takenobu, J. Takeya, and Y. Iisawa, Appl. Phys. Lett. **88**, 033505 (2006).
[12] J. Takeya, J. Kato, K. Hara, M. Yamagishi, R. Hirahara, K. Yamada, Y. Nakazawa, S. Ikehata, K. Tsukagoshi, Y. Aoyagi, T. Takenobu, and Y. Iwasa, Phys. Rev. Lett. **98**, 196804 (2007).
[13] M. Yamagishi, J. Takeya, Y. Tominari, Y. Nakazawa, T. Kuroda, S. Ikehata, M. Uno, T. Nishikawa, and T. Kawase, Appl. Phys. Lett. **90**, 182117 (2007).
[14] B. D. Chapman, A. Checco, R. Pindak, T. Siegrist, and C. Kloc, J. Cryst. Growth **290**, 479 (2006).
[15] O. D. Jurchescu, A. Meetsma, and T. T. Palstra, Acta Crystallogr., Sect. B: Struct. Sci. **62**, 330 (2006).
[16] M. Needels, J. D. Joannopoulos, Y. Bar-Yam, and S. T. Pantelides, Phys. Rev. B **43**, 4208 (1991).
[17] L. Tsetseris, D. M. Fleetwood, R. D. Schrimpf, X. J. Zhou, I. G. Batyrev, and S. T. Pantelides, Microelectron. Eng. **84**, 2344 (2007).
[18] D. Käfer and G. Witte, Phys. Chem. Chem. Phys. **7**, 2850 (2005).
[19] O. Mitrofanov, D. V. Lang, C. Kloc, J. M. Wikberg, T. Siegrist, W. Y. So, M. A. Sergent, and A. P. Ramirez, Phys. Rev. Lett. **97**, 166601 (2006).
[20] C. Krellner, S. Haas, C. Goldmann, K. P. Pernstich, D. J. Gundlach, and B. Batlogg, Phys. Rev. B **75**, 245115 (2007).
[21] M. Kytka, A. Gerlach, F. Schreiber, and J. Kovac, Appl. Phys. Lett. **90**, 131911 (2007).
[22] W. So, J. M. Wikberg, D. V. Lang, O. Mitrofanov, C. L. Kloc, T. Siegrist, A. M. Sergent, and A. P. Ramirez, Solid State Commun. **142**, 483 (2007).
[23] J. E. Northrup and M. L. Chabinyc, Phys. Rev. B **68**, 041202(R) (2003).
[24] L. Tsetseris and S. T. Pantelides, Phys. Rev. B **75**, 153202 (2007).
[25] J. P. Perdew and A. Zunger, Phys. Rev. B **23**, 5048 (1981).
[26] D. Vanderbilt, Phys. Rev. B **41**, 7892 (1990).
[27] G. Kresse and J. Furthmuller, Phys. Rev. B **54**, 11169 (1996).
[28] D. J. Chadi and M. L. Cohen, Phys. Rev. B **8**, 5747 (1973).
[29] O. Jepson and O. K. Andersen, Solid State Commun. **9**, 1763 (1971).
[30] D. A. da Silva Filho, E. G. Kim, and J. L. Brédas, Adv. Mater. (Weinheim, Ger.) **17**, 1072 (2005).
[31] D. V. Lang, X. Chi, T. Siegrist, A. M. Sergent, and A. P. Ramirez, Phys. Rev. Lett. **93**, 086802 (2004).
[32] L. Tsetseris and S. T. Pantelides, Appl. Phys. Lett. **87**, 233109 (2005).